



# Wavelength-dependent Extinction and Grain Sizes in “Dippers”

Michael L. Sitko<sup>1</sup> , Ray W. Russell<sup>2</sup> , Zachary C. Long<sup>3</sup>, Korash Assani<sup>3</sup>, Monika Pikhartova<sup>3</sup> , Ammar Bayyari<sup>3,4</sup>, Carol A. Grady<sup>5</sup>, Carey M. Lisse<sup>6</sup> , Massimo Marengo<sup>7</sup> , John P. Wisniewski<sup>8</sup> , and William C. Danchi<sup>9</sup>

<sup>1</sup>Center for Exoplanetary Systems, Space Science Institute, 4750 Walnut Street, Suite 205, Boulder, CO 80301, USA; [sitko@spacescience.org](mailto:sitko@spacescience.org)

<sup>2</sup>The Aerospace Corporation, Los Angeles, CA, USA

<sup>3</sup>Department of Physics, University of Cincinnati, Cincinnati, OH 45221-0011, USA

<sup>4</sup>Department of Physics and Astronomy, University of Hawaii, 2505 Correa Road Watanabe 416, Honolulu, HI 96822, USA

<sup>5</sup>Eureka Scientific, Inc., 2452 Delmer Street, Suite 100, Oakland, CA 496002, USA

<sup>6</sup>JHU-APL, 11100 Johns Hopkins Road, Laurel, MD 20723, USA

<sup>7</sup>Department of Physics and Astronomy, Iowa State University, Ames, IA 50010, USA

<sup>8</sup>Department of Physics and Astronomy, George Mason University, 4400 University Drive, Fairfax, VA 22030-4444, USA

<sup>9</sup>NASA Goddard Space Flight Center, 8800 Greenbelt Road, Greenbelt, MD 20771-2400, USA

Received 2019 July 9; revised 2023 March 1; accepted 2023 March 15; published 2023 June 23

## Abstract

We have examined internight variability of K2-discovered “dippers” that are not close to being viewed edge-on, as determined from previously reported ALMA images, using the SpeX spectrograph on NASA’s Infrared Telescope Facility. The three objects observed were EPIC 203850058, EPIC 205151387, and EPIC 204638512 (=2MASS J16042165-2130284). Using the ratio of the fluxes between two successive nights, we find that for EPIC 204638512 and EPIC 205151387, we find that the properties of the dust differ from that seen in the diffuse interstellar medium and denser molecular clouds. However, the grain properties needed to explain the extinction does resemble those used to model the disks of many young stellar objects. The wavelength-dependent extinction models of both EPIC 204638512 and EPIC 205151387 includes grains at least 500  $\mu\text{m}$  in size, but lacks grains smaller than 0.25  $\mu\text{m}$ . The change in extinction during the dips, and the timescale for these variations to occur, imply obscuration by the surface layers of the inner disks. The recent discovery of a highly misinclined inner disk in EPIC 204638512 suggests that the variations in this disk system may point to due to rapid changes in obscuration by the surface layers of its inner disk, and that other “face-on” dippers might have similar geometries. The He I line at 1.083  $\mu\text{m}$  in EPIC 205151387 and EPIC 20463851 were seen to change from night to night, suggesting that we are seeing He I gas mixed in with the surface dust.

*Unified Astronomy Thesaurus concepts:* [Protoplanetary disks \(1300\)](#); [Protostars \(1302\)](#); [Circumstellar dust \(236\)](#)

*Supporting material:* data behind figure

## 1. Introduction

The formation of planets in young protoplanetary disk systems by means of core accretion requires that the dust within these systems undergo growth and likely settling of the largest grains toward the disk midplane. The degree of such grain growth, however, is often difficult to assess observationally. At visible- to mid-infrared wavelengths, the disks may be optically thick, and observations only give clues about the surface layers. Both the scattered light and thermal emission are subject to the effects of radiative transfer, and their interpretation will be model dependent. At millimeter/submillimeter wavelengths, the spectral slope provide clues as to grain sizes, but optical thickness and grain size distributions will not be constant throughout the planet-forming regions of the disk. In particular, gas/dust mass ratios derived from such grains seem to unusually low (by factors of up to 30 times compared to expected gas/dust ratios; Burstiel et al. 2010; Williams & Best 2014; Kama et al. 2016; Long et al. 2017). Recent models of the depletion of CO in young disk systems suggests that gaseous CO will condense into ices, and coat more refractory grains, and the extent of the depletion depends on radial distance and age of the system (McClure et al. 2016; Powell

et al. 2022). Mid-infrared interferometry near 10  $\mu\text{m}$  indicates that grains are often larger near the star than further out (van Boekel et al. 2004; Lopez et al. 2022).

Occultations of the stellar light by dust along the line of sight, however, can provide a more direct measure of the wavelength-dependent extinction of the dust in these systems at visible and near-IR wavelengths. Many young stars undergo variations in brightness that are most easily explained by dust extinction in the upper layers of disks that are viewed at high inclinations. Such “UX Orionis” stars, or “UXors,” have been known for some time (Grinin et al. 1991, 1996; Eaton & Herbst 1995). In the case of disks with puffed-up inner rims (Natta et al. 2001; Dullemond & Dominik 2004) the occulting dust would likely be located at the inner disk rim of highly self-shadowed disks (Dullemond et al. 2003). The color changes in these systems have been studied at visible wavelengths, and as expected for submicron-sized grains, the extinction is accompanied by reddening, until the dust becomes optically thick, after which “bluing” may actually occur due to the remaining stellar light reaching the observer relatively unaffected. This occurs when the disk is very optically thick, but scattering at the poles reaches the observer (Grinin et al. 1991).

The Spitzer Infrared Array Camera and the Convection, Rotation, and Planetary Transit satellite provided long time baseline photometric observations of large numbers of Classical T Tauri stars in young stellar clusters. Among these were stars exhibiting large irregular changes in brightness over



Original content from this work may be used under the terms of the [Creative Commons Attribution 4.0 licence](#). Any further distribution of this work must maintain attribution to the author(s) and the title of the work, journal citation and DOI.

**Table 1**  
Dipper Fundamental Parameters

Star Name	EPIC 203850058	EPIC 204638512	EPIC 205151387
Dippers			
2MASS	16253849–2613540	016042165–2130284	16090075–1908526
Gaia DR3	6049072316675781120	6243393817024157184	6245777283349430912
Star properties			
Gaia distance (pc)	141.577	145.309	137.397
Spectral type	M5	K2	M0.5
$P_{\text{rot}}$ (days)	2.88	5.0	9.55
Region	$\rho$ Oph	Upper Sco	Upper Sco
$K$ -band magnitude	10.766	8.508	9.475
Disk properties			
ALMA disk diam. ( $''$ )	$0.2 \times 0.3$	1	$0.6 \times 0.4$
ALMA disk diam. (au)	$28.3 \times 42.5$	145	$82.2 \times 54.8$
ALMA disk incl. ( $^{\circ}$ )	$73 \pm 23$	$6 \pm 1.5$	$53 \pm 2$
Disk type <sup>a</sup>	Full	Transitional	Full
Age	1 Myr	10 Myr	10 Myr

**Note.**

<sup>a</sup> (Ansdell et al. 2016a).

timescales of days or even hours. These “dippers” became important targets for the K2 mission, and Ansdell et al. (2016a) reported finding many in the Upper Sco and  $\rho$  Oph stellar associations. Similar dipper activity was observed in stars in the young star-formation region NGC 2264 (Stauffer et al. 2016). While disks with near edge-on orientations would be most likely capable of occulting the light of the star, Ansdell et al. (2016b) presented ALMA continuum observations of three dippers, EPIC 203850058, EPIC 205151387, and EPIC 204638512, whose geometries were far from edge-on. In the case of EPIC 204638512, the disk is nearly face-on ( $\sim 6^{\circ} \pm 1^{\circ}.5$ ), with a large dust cavity, yet it exhibits brightness fluctuations of nearly 1 mag over a time span of a day. This suggests that if the brightness changes were due to dust, a UXor-type geometry was unlikely.

However, recent imaging data for EPIC 204638512 ALMA (Mayama et al. 2018) and VLT/SPHERE (Pinilla et al. 2018) provide evidence for an inner disk that is misaligned with the outer disk. With ALMA observations, a twisted “butterfly” radial velocity map in CO (3–2) clearly shows a highly inclined inner disk, despite the outer disk being seen nearly face-on. Shadows of the inner disk cast on the outer disk are also visible in both dust continuum thermal emission and gas emission maps. These shadows are also visible in the scattered light images from SPHERE, where the depth and width of the shadows change with time. In the case of this dipper, at least, the light variations are likely coming from irregularities in the orbiting dust in the inner disk. In the other two objects discussed in this paper, we need more evidence to conclude a similar geometry, because there are other ways to generate similar variability in brightness.

Other possible mechanisms may also produce somewhat similar changes in the observed brightness of a star. Using high-spatial-resolution imaging obtained with the Goddard Fabry–Pérot imager on the Apache Point Observatory 3.5 m telescope, Wassell et al. (2006) reported a string of luminous clouds along two opposing outflows in the Herbig Ae star HD 163296 (MWC 275). Ellerbroek et al. (2014), using photometry obtained by the All Sky Automated Survey (Pojmanski 1997), reported that a dipper-like extinction event occurred in 2001 in the star, and this extinction event was

traced, using the measured proper motion of these clouds, to an ejection event at that time. It was suggested that dust entrained in a disk wind (see their Figure 9), similar to that suggested by Bans & Königl (2012) for the source of the near-IR emission in protostellar systems, was the cause. Unfortunately, the ASAS photometric observations provided no color information. However, in 2012 multifilter observations obtained by the American Association of Variable Star Observers captured a 1 day extinction event that could be subjected to modeling using various types of grains. Grains typical of both the diffuse interstellar medium and dark molecular clouds with star-formation regions provided poor fits to the wavelength dependence of the extinction. However grains that had undergone further growth, and were similar to those included in some radiative transfer models of disks, such as those used in the HOCHUNK3D code package by Whitney et al. (2013), were more successful at reproducing the extinction properties of that one-day event Pikhartova et al. (2021).

Here we report near-infrared observations of the three dippers in Ansdell et al. (2016b) obtained with the SpeX spectrograph on NASA’s Infrared Telescope facility (IRTF) taken on two consecutive nights. From these we obtain the extinction curves for the two brighter dippers, and subject them to the same extinction analysis that Pikhartova et al. (2021) employed for HD 163296.

## 2. Observations

We observed the three “face-on” dippers (see Table 1) on two successive nights, 2017 August 10 and 11, at an effective spectral resolution  $R = 750$  ( $0''.8$  slit) from 0.7 to 2.4  $\mu\text{m}$  using the SXD grating of the SpeX spectrograph (Rayner et al. 2003) on NASA’s IRTF. In order to determine the absolute fluxes of these slit spectra, which are subject to time-variable throughput due to the effects of astronomical seeing and telescope guiding, we also observed them in the  $K$  band using the SpeX guide camera using a 9 point dither pattern (Table 2). Both spectra and images were flux calibrated using the A0V star HD 145127 at nearly the same airmass. The spectral data reduction was carried out using the Spextool software, running under IDL (Vacca et al. 2003; Cushing et al. 2004).

**Table 2**  
Observed Dipper *K*-band Fluxes<sup>a</sup>

Date (UT)	MJD	EPIC 203850058	MJD	EPIC 204638512	MJD	EPIC 205151387
170810	57975.23912	0.65(0.11)	57975.25421	3.95(0.12)	57975.27806	2.34(0.11)
170811	57976.24319	0.60(0.05)	57976.24319	4.80(0.04)	57976.27624	2.01(0.04)

**Note.**

<sup>a</sup> *K*-band flux is  $\lambda F_{\lambda}$  in units of  $10^{-13} \text{ W m}^{-2}$ . Uncertainties are given in parentheses.

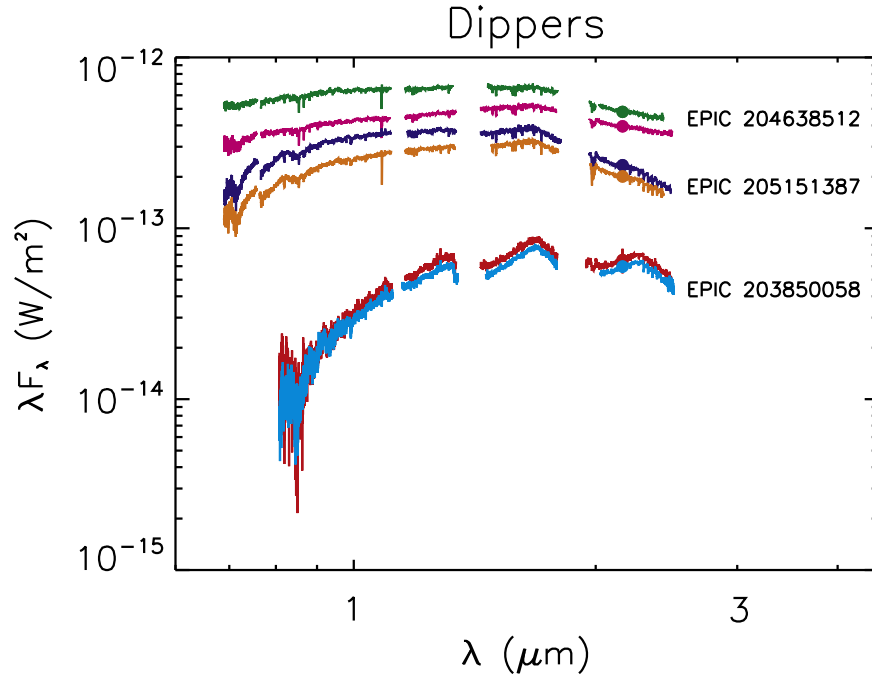


**Figure 1.** 0.7–2.4  $\mu\text{m}$  spectra of three dippers obtained with the SpeX spectrograph between 0.7 and 2.4  $\mu\text{m}$  on 2017 August 10 and 11 (UT). Due to poor signal/noise, the spectrum of EPIC 203850058 was truncated at wavelengths smaller than 0.8  $\mu\text{m}$ . The spectra were calibrated in absolute flux using *K*-band images obtained with the guide camera (filled circles). For EPIC 204628512 and EPIC 205151387, the fainter spectrum was also slightly redder, and were used to examine the wavelength dependence of the extinction (reddening). The difference in the flux levels for EPIC 203850058 were so small that we did not attempt to derive a flux ratio for examining potential reddening by dust.

(The data used to create this figure are available.)

In Figure 1 we show the SpeX spectra of all three dippers, each normalized by the *K*-band fluxes. The two brightest dippers, EPIC 204638512 (K2; Köhler et al. 2000) and EPIC 205151387 (M0.1V; Ansdell et al. 2016a), underwent marked changes in brightness between the two nights, while the third, much fainter one, EPIC 203850058 (M5; Manora et al. 2015), showed smaller changes, being less than the “noise” at the shortest wavelengths.

### 3. Wavelength-dependent Extinction

To characterize the dust we first selected the brightest of these objects, EPIC 204638512 (=2MASS J16042165-2130284), an object that has been the target of imaging programs using extreme adaptive optics (Canovas et al. 2017; Dong et al. 2017; Uyama et al. 2017). The difference in extinction between the two successive nights (we cannot assume that the brighter flux state has no extinction) was determined by taking the ratio of the two flux-calibrated spectra, and comparing the result with a number of published dust extinction laws, as shown in Figure 2.

We began with the extinction laws of Cardelli et al. (1989) often used in the literature for reproducing extinction by dust in

the diffuse interstellar medium. Despite changing the ratio of total-to-selective extinction ( $R_V$ ) where larger values represent larger grains), no good fit was obtained. Other recipes for denser cloud regions (Weingartner & Draine 2001; McClure 2009) fared little better.

Next we tried grain prescriptions (e.g., from Cotera et al. 2001 and Wood et al. 2002) developed for circumstellar disks and included in the HOCHUNK3D Monte Carlo radiative transfer code of Whitney et al. (2013). These use the optical constants of silicates and carbonaceous grains from Rouleau & Martin (1991) and Weingartner & Draine (2001). “www03” refers to the grain created to the disk midplane providing the best fit for the SED of HH30 in Wood et al. (2002). Specifically, their Model 1, which uses a mixture of amorphous carbon and astronomical silicates that have a power-law size distribution  $n(a) \sim a^{-p}$  with  $p = 3.0$ , plus exponential cutoff starting at 50  $\mu\text{m}$  and going to longer wavelengths, to a grain maximum size of 1000  $\mu\text{m}$ . “ww04” is the grain model of Cotera et al. (2001), used to fit the scattered light in HH30. It a power-law index of 3.5 for amorphous carbon and 3.0 for silicates, a turnover at 0.55  $\mu\text{m}$  and grain maximum of 20  $\mu\text{m}$ . “ww002” is

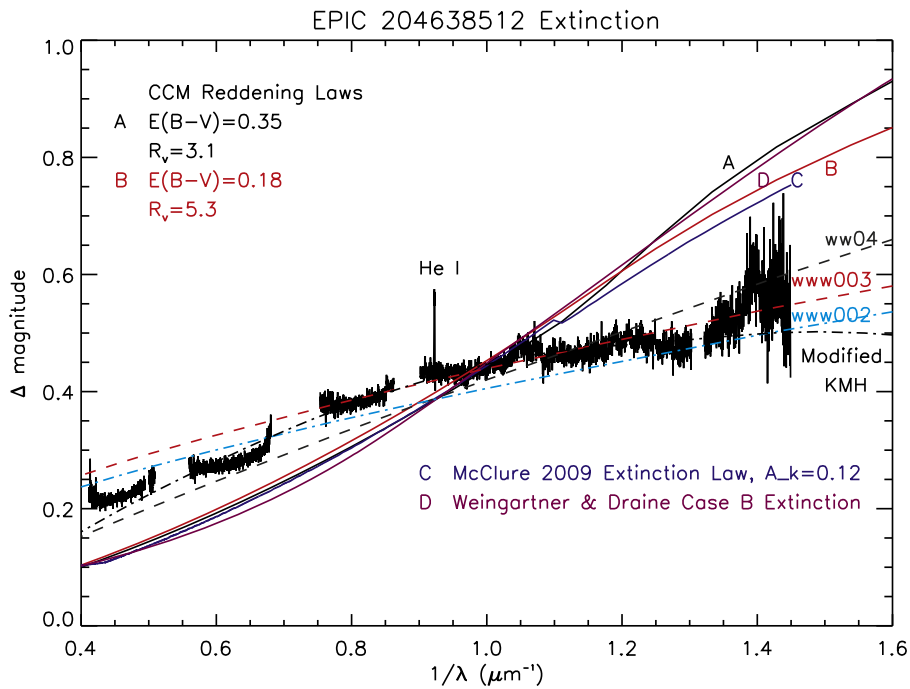


**Figure 2.** Extinction curve of EPIC 204638512. The model curves labeled “CCM” are those of Cardelli et al. (1989), using different values of  $R_V$ , and representative of ISM extinction. Also shown are DMC extinction curves from McClure (2009) and Weingartner & Draine (2001). The curves labeled “ww04,” “www003,” and “www002” are grain files included with the HOCHUNK3D code package of Whitney et al. (2013). For example, “www003” is Model 1 of Wood et al. (2002), which has a power-law grain size distribution, with a maximum grain size of  $1000 \mu\text{m}$  and an exponential cutoff at starting an  $50 \mu\text{m}$  and going to the large grain limit. “Modified KMH” uses the grain size distribution of Kim et al. (1994) but increasing the minimum and maximum grain sizes to  $0.25 \mu\text{m}$  and  $500 \mu\text{m}$ , respectively. These are described more fully in the text.

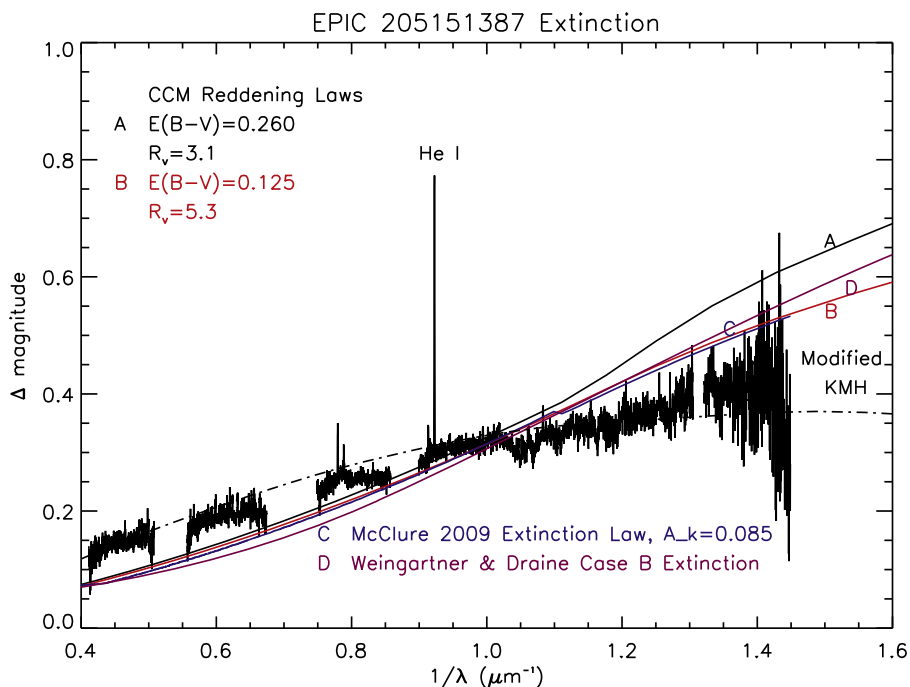


**Figure 3.** Extinction curve of EPIC 205151387. The grain models are explained in the caption to Figure 2, except we did not include grain models used in the HOCHUNK3D package; however, it is clear that the grain sizes involved are similar to those in EPIC 204638512. The change in the He I feature is more pronounced in EPIC 205151387.

the same grain model as “w003” except having the exponential cutoff at  $100 \mu\text{m}$  instead of  $50 \mu\text{m}$ .

Finally we used a similar grain file that used the ISM dust extinction of Kim et al. (1994) but adjusted the minimum and maximum size present. This extinction (“Modified KMH”) has

grains extending to at least  $500 \mu\text{m}$  and lacks grains smaller than  $0.25 \mu\text{m}$ . While larger grains were not excluded, they produced little further change in the resulting extinction at the observed wavelengths.

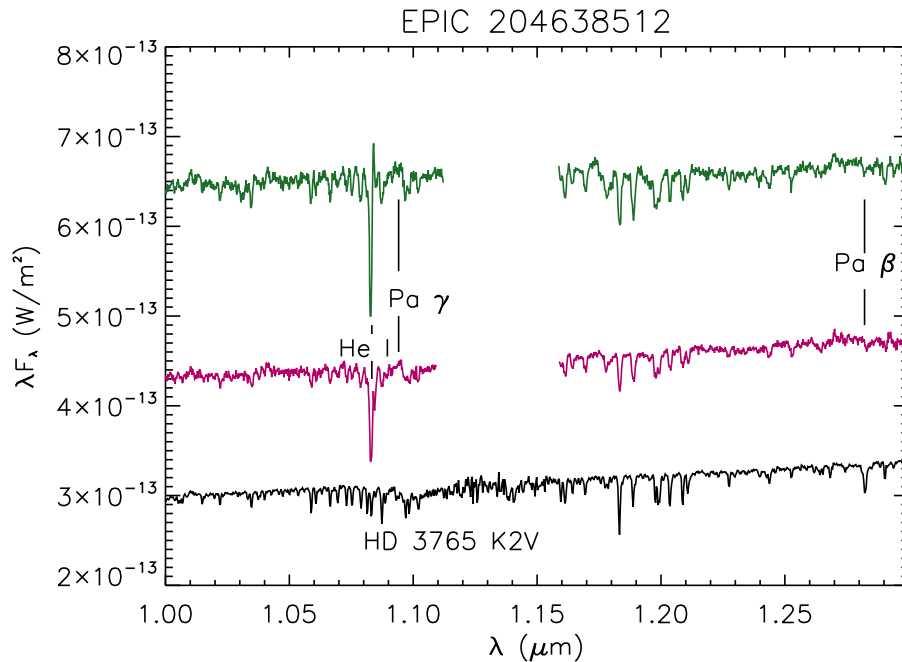


**Figure 4.** The region near He I line for EPIC 204638512 on two consecutive nights, along with the spectrum of HD 3765, a star of similar spectral type, taken from the SpeX Atlas of Cool Stars (Rayner et al. 2009). The gap in the data on EPIC 204628512 is the result of trimming out the spectrum heavily affected by telluric absorption. Also shown are the locations of two nearby hydrogen lines, often seen in emission in stars actively accreting material from their disks, and the He I line. The Pa  $\beta$  line is weaker than in HD 3765, suggesting it might be weakly in emission, partially filling the photospheric absorption line (in K2 V stars this region also contains a blend of Ti I, Ni I, Fe I, and Ca I lines—see Figure 30 of Rayner et al. 2009). In the brighter continuum state, the He I line exhibits a weak emission component in addition to a strong absorption core at shorter wavelengths. This resembles a P Cygni-like profile, but with a relatively stronger short wavelength absorption component. In the higher dust occultation data, the red wing of the He I line is not evident.

We also subjected the extinction curve of EPIC 205151387 to a similar analysis, as illustrated in Figure 3. This uses the same modified KMH model as in the case of EPIC 204638512 (with lower total extinction), grains more consistent with those used in disk modeling provided a much better agreement with the observed extinction than did either ISM-like or dark cloud-like extinction models.

A similar analysis was applied to a short-duration extinction event in HD 163296 by Pikhartova et al. (2021). In the case of HD 163296, an extinction event lasting only about 1 day was modeled, with the wvw003 grain model providing the best fit overall. The large extinction event of 2001 (Ellerbroek et al. 2014), likely due to the ejection of HH-like blobs in a bipolar jet (with a disk wind) was mostly monitored at a single visible wavelength, and could not be subjected to the same wavelength-dependent extinction analysis.

#### 4. The Gas

In both derived extinction curves, there is an added feature at a wavelength consistent with the He I line at  $1.083 \mu\text{m}$  often seen in other young stellar objects. In EPIC 204638512, this line seems to exhibit a “P Cygni” profile (blueshifted absorption component flanked by a redshifted emission component) indicative of outflowing gas (with the blue absorption wing being produced by gas between the observer and the stellar photosphere), but the evidence is only suggestive (see Figure 4). Silicia-Aguilar et al. (2020) reported line profile changes in  $H\alpha$  and  $H\beta$ . The former line exhibited complex behavior, with epochs of inflowing and outflowing gas, while the latter had one epoch with a very distinct inflowing gas component. In EPIC 205251387 (Figure 5), the He I line is more indicative of infalling gas. In PMS stars, the He I profile

can exhibit strong time-dependent changes in intensity and shape (Sitko et al. 2012; Fernandes et al. 2018). A significant fraction of the time, HD 163296 seems to exhibit a combination of both outflowing and inflowing gas (Pikhartova et al. 2021) at the same time. The data on EPIC 203850058 (Figure 6) was deemed to be of insufficient quality to determine the nature of the gas flow characteristics.

For completeness, we also show the two spectra of EPIC 203850058 (Figure 5), but the data were of insufficient quality for an analysis of the extinction.

#### 5. Discussion

Using ALMA dust continuum and CO line emission data of EPIC 204638512, Mayama et al. (2018) have provided convincing evidence of an inner disk that is misaligned from the outer disk, with an inclination of  $-45^\circ$ . Pinilla et al. (2018) have also found that the shadows cast by the inner disk onto the outer disk are variable in time. These results clearly indicate that the dipper phenomenon EPIC 204638512 are due to dust in the inclined inner disk producing variable extinction by the inclined inner disk. While less-well studied, it suggests that the extinction events seen in EPIC 205251387 have a similar origin.

In this paper we have derived the extinction properties of the dust in these two sources that imply grains that are unlike those found in the general ISM from which they originally formed. Rather, the occulting grains are those that at some earlier epoch have undergone significant growth in size. Such grain growth is expected in disks (D’Alessio et al. 2001, 2006; Ferlan et al. 2005), and is generally thought to be accompanied by settling of the larger grains to the disk midplane, as they begin to decouple from the gas. In the case of EPIC 205151387 and

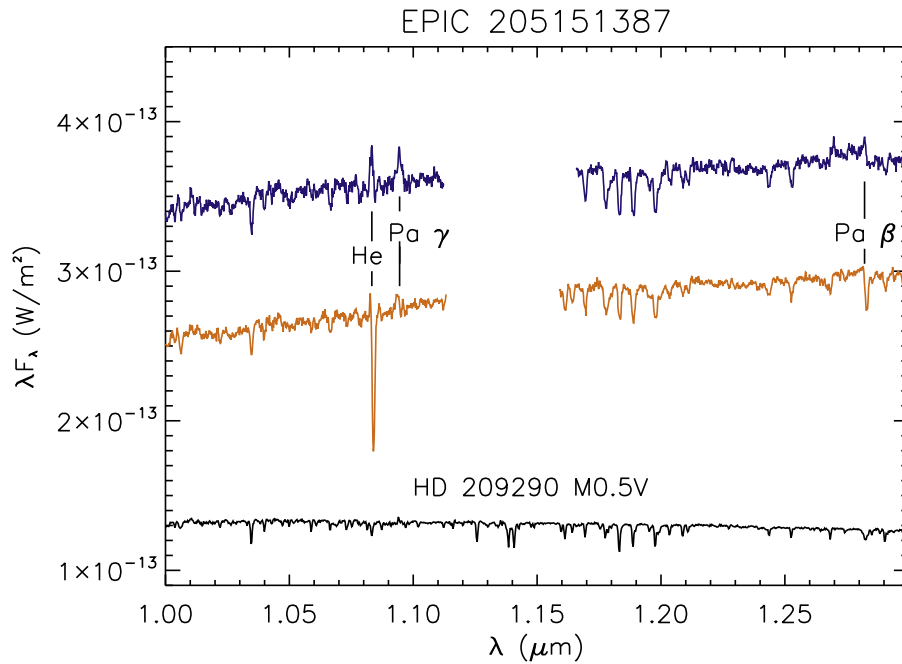


**Figure 5.** The region near He I line for EPIC 205151387 on two consecutive nights, along with the spectrum of HD 209290, a star of similar spectral type, taken from the SpeX Atlas of Cool Stars (Rayner et al. 2009). During the dust extinction event (lower net flux), the He I absorption line became even stronger than in EPIC 204628512. The Pa  $\beta$  line developed a distinct absorption component, and the emission on Pa  $\gamma$  was weakened. The absorption in He I and Pa  $\beta$  are both shifted toward longer wavelengths than the emission, inverse P Cygni-like profiles, indicating infalling gas.

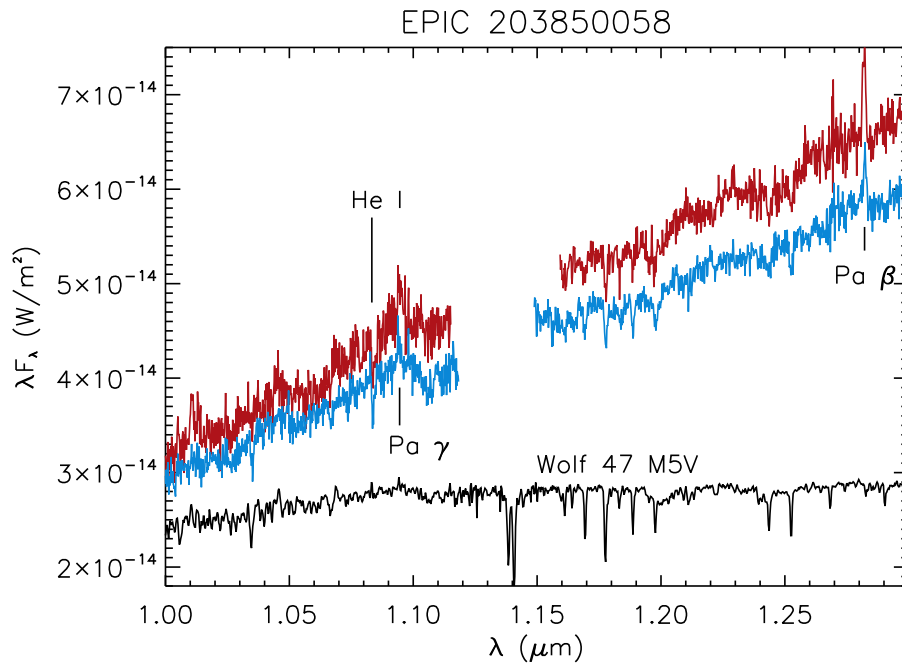


**Figure 6.** The region near He I line for EPIC 203850058 on two consecutive nights, along with the spectrum of Wolf 47, a star of similar spectral type, taken from the SpeX Atlas of Cool Stars (Rayner et al. 2009). The Pa  $\beta$  and Pa  $\gamma$  lines are in emission, suggesting some accreting gas. The He I line exhibits absorption, but unlike EPIC 204638512 and EPIN 501551387, does not show a detectable He I emission component, although the quality of the spectra are inferior to those of the other two dippers. Note that Wolf 47 is a dMe star exhibiting flares (including at radio wavelengths; White et al. 1989) and so some line emission (Pa  $\gamma$ ?) is not unexpected.

EPIC 204638512, the types of grains present are consistent with the sorts of grains expected in disk systems. Indeed, the extinction properties of the grains used were *derived* from the scattered light and thermal emission of the disk of HH30 (Cotera et al. 2001; Wood et al. 2002). However, if the dust particles causing the dipper events are this large, then the “settled dust” dominates these extinction events. In this case we may be seeing one possible near-final evolutionary stage of a

disk system. The structure of the CO maps in EPIC 204638512 might also hint at infalling material (Mayama et al. 2018), but the evidence is inconclusive. The evidence seems stronger that this system possesses a misinclined inner disk that produces variable amounts of shadowing nearly  $140^{\circ}$ – $180^{\circ}$  apart in azimuth in the outer disk. Dipper occultation events would be more likely than if the inner regions had the low inclinations originally reported for the outer disk (Ansdell et al. 2016b).

While the dipper events are almost inevitable for highly inclined inner disks, is there evidence for similar structure in disks not fortuitously observed at high inclination? A number of disks exhibit outer disk shadows that imply misaligned inner disks: HD 142527 (Avenhaus et al. 2014), HD 100453 (Benisty et al. 2017; Long et al. 2017), TW Hya (Debes et al. 2017; Poteet et al. 2018), and HD 100453 (Garufi et al. 2016). A related type of phenomenon might also be occurring in the nondipper star SAO 206462 (HD 135344B). Recent SPHERE imaging of its disk by Stolker et al. (2017) showed *moving shadows* in the outer disk. These traveled many degrees in the course of months, suggesting varying shadows by irregular dust clouds in the inner disk. This apparent orbital motion was accompanied by changes in color of the disk in general, suggesting that the outer disk was experiencing changing illumination due to clouds that effectively reddened the light reaching it. Were its inner disk highly inclined with respect to the viewer, it might exhibit dipper-like events. Careful monitoring of near-IR spectra of systems with evidence for misaligned inner disks should be pursued.

## 6. Conclusions

We have found that the “dipper” events observed in EPIC 20435638512 are due to changes in the extinction by dust grains whose sizes indicate significant grain growth compared to their ISM sizes, and these are located in the surface layers of an inner disk that is highly inclined to the outer disk, seen in ALMA continuum images. Our results also suggest that other dippers having outer disks with modest inclinations (such as EPIC 205151387, with  $i = 53^\circ \pm 2^\circ$  might contain misaligned inner disks). The detection of shadows, especially those with wide position angle separations and/or variable shadows in the outer disk would help confirm such an hypothesis, as would interferometric observations of the inner regions.

As to the gas velocity structures in EPIC 204638512 and EPIC 205151387, the situation is complex. Both outflowing (wind) and inflowing (accretion) gas is present in differing degrees at different epochs. Further work that includes a number of emission/absorption lines simultaneous with thermal dust extinction measurements are needed.

This paper was based on observations taken with the IRTF/SpeX 0.8–5.5  $\mu\text{m}$  Medium-Resolution Spectrograph and Imager, funded by the National Science Foundation and NASA and operated by the NASA Infrared Telescope Facility. The authors would like to thank the tireless support of the staff of NASA’s Infrared Telescope Facility. We wish to emphasize the pivotal cultural role and reverence that the summit of Maunakea has always had within the indigenous Hawaiian community. We are most fortunate to have the privilege to conduct scientific observations from this mountain. This work was supported in part by NASA XRP grants NNX17AF88G, NNX16AJ75G (MLS), and 80NSSC20KO254 (CAG).

*Software:* HOCHUNK3D (Whitney et al. 2013), Spextool (Vacca et al. 2003; Cushing et al. 2004).

## ORCID iDs

Michael L. Sitko  <https://orcid.org/0000-0003-1799-1755>

Ray W. Russell  <https://orcid.org/0000-0002-7818-2305>  
 Monika Pikhartova  <https://orcid.org/0000-0002-6767-6377>  
 Carey M. Lisse  <https://orcid.org/0000-0002-9548-1526>  
 Massimo Marengo  <https://orcid.org/0000-0001-9910-9230>  
 John P. Wisniewski  <https://orcid.org/0000-0001-9209-1808>  
 William C. Danchi  <https://orcid.org/0000-0002-9209-5830>

## References

- Ansdell, M., Gaidos, E., Rappaport, S. A., et al. 2016a, *ApJ*, 816, 69  
 Ansdell, M., Gaidos, E., Williams, J. P., et al. 2016b, *MNRAS*, 462, L101  
 Avenhaus, H., et al. 2014, *ApJ*, 790, 56  
 Benisty, M., Stolker, T., Pohl, A., et al. 2017, *A&A*, 597, A42  
 Burstiel, T., Ricci, L., Trotta, F., et al. 2010, *A&A*, 516, L14  
 Bans, A., & Königl, A. 2012, *ApJ*, 758, 100  
 Canovas, H., Hardy, A., Zurlo, A., et al. 2017, *A&A*, 598, A43  
 Cardelli, J. A., Clayton, G. C., & Mathis, J. S. 1989, *ApJ*, 345, 245  
 Cotera, A.-S., Whitney, B. A., Young, E., et al. 2001, *ApJ*, 556, 958  
 Cushing, M. C., Vacca, W. D., & Rayner, J. T. 2004, *PASP*, 116, 362  
 D’Alessio, P., Calvet, N., & Hartmann, L. 2001, *ApJ*, 553, 321  
 D’Alessio, P., Calvet, N., Hartmann, L., Franco-Hernández, R., & Servín, H. 2006, *ApJ*, 638, 314  
 Debes, J. H., Poteet, J., Jang-Condell, H., et al. 2017, *ApJ*, 835, 205  
 Dong, R., van der Marel, N., Hashimoto, J., et al. 2017, *ApJ*, 836, 201  
 Dullemond, C. P., & Dominik, C. 2004, *A&A*, 417, 159  
 Dullemond, C. P., van den Ancker, M. E., Acke, B., & van Boekel, R. 2003, *ApJL*, 594, L47  
 Eaton, N. L., & Herbst, W. 1995, *AJ*, 110, 2369  
 Ellerbroek, L. E., Podio, L., Dougados, et al. 2014, *A&A*, 563, A87  
 Fernandes, R. B., Long, Z. C., Pikhartova, M., et al. 2018, *ApJ*, 856, 103  
 Ferlan, E., Calvet, N., D’Alessio, P., et al. 2005, *ApJL*, 628, L65  
 Garufi, A., et al. 2016, *A&A*, 588, A8  
 Grinin, V. P., Kiselev, N. N., & Minikulov, N. 1991, *Ap&SS*, 186, 283  
 Grinin, V. P., Kozlova, O. V., Thé, P. S., & Rostopchina, A. N. 1996, *A&A*, 309, 474  
 Kama, M., Bruderer, S., Carney, M., et al. 2016, *A&A*, 588, A108  
 Kim, S. H., Martin, P. G., & Hendrey, P. D. 1994, *ApJ*, 422, 164  
 Köhler, R., Kunkel, M., Leinert, C., & Zinnecker, H. 2000, *A&A*, 356, A541  
 Long, Z. C., Fernandes, R.B., Sitko, M.L., et al. 2017, *ApJ*, 838, 62  
 Lopez, B., Lagarde, S., Petrov, R.G., et al. 2022, *A&A*, 659, A192  
 Manora, C. F., Testi, L., Natta, A., & Alcalá, J. M. 2015, *A&A*, 579, A66  
 Mayama, S., Akiyama, E., Panić, O., et al. 2018, *ApJL*, 868, L3  
 McClure, M. 2009, *ApJL*, 693, L81  
 McClure, M. K., Bergin, E.A., Cleeves, L.I., et al. 2016, *ApJ*, 831, 167  
 Natta, A., Prusti, T., Neri, R., et al. 2001, *A&A*, 371, 186  
 Pikhartova, M., Long, Z.C., Assani, K.D., et al. 2021, *ApJ*, 919, 64  
 Pinilla, P., Benisty, M., de Boer, J., et al. 2018, *ApJ*, 868, 85  
 Pojmanski, G. 1997, *AcA*, 47, 467  
 Poteet, C. A., Chen, C.H., Hines, D.C., et al. 2018, *ApJ*, 860, 115  
 Powell, D., Gao, P., Murrey-Clay, R., & Zhang, X. 2022, *NatAs*, 6, 1147  
 Rayner, J. T., Toomey, D. W., Onaka, P. M., et al. 2003, *PASP*, 115, 362  
 Rayner, J. T., Cushing, M. C., & Vacca, W. D. 2009, *ApJS*, 185, 289  
 Rouleau, F., & Martin, G. G. 1991, *ApJ*, 377, 526  
 Silicia-Aguilar, A., Manara, C.F., de Boer, J., et al. 2020, *A&A*, 633, A37  
 Sitko, M. L., Day, A. N., Kimes, R. L., et al. 2012, *ApJ*, 745, 29  
 Stauffer, J., Cody, A.M., McGinnis, P., et al. 2015, *AJ*, 149, 130  
 Stolker, T., Sitko, M., Lazareff, B., et al. 2017, *ApJ*, 849, 143  
 Uyama, T., Hashimoto, J., Kuzuhara, M., et al. 2017, *AJ*, 153, 106  
 Vacca, W. D., Cushing, M. C., & Rayner, J. T. 2003, *PASP*, 115, 389  
 van Boekel, R., Min, M., Leinert, Ch. W., et al. 2004, *Natur*, 432, 479  
 Wassell, E. J., Grady, C. A., Woodgate, B., Kimble, R. A., & Bruhweiler, F. C. 2006, *ApJ*, 650, 985  
 Weingartner, J. C., & Draine, B. T. 2001, *ApJ*, 548, 296  
 White, S. M., Jackson, P. D., & Kundu, M. R. 1989, *ApJS*, 71, 895  
 Whitney, B. A., Robitaille, T. P., Bjorkman, J. E., et al. 2013, *ApJS*, 207, 30  
 Williams, J., & Best, W. M. J. 2014, *ApJ*, 788, 59  
 Wood, K., Wolff, M. J., Bjorkman, J. E., & Whitney, B. 2002, *ApJ*, 564, 887